Supporting Information

Fan *et al.* 10.1073/pnas.0800980105

SI Text

Methods. ***Plant material and growth conditions.*** All transgenics were in the Columbia (Col-0) ecotypic background. An EMS-generated mutant line (*agb1-1*), T-DNA insertional mutant lines (*agb1-2*, *gpa1-4*, *rgs1-1*, *rgs1-2*), and *gpa1-4 agb1-2* double mutant lines have been described previously. pGWB42 vector (pGWB1:35S:YFP) was used to generate AGB1 overexpressing lines (AGB1-OXs; construct was pGWB42:AGB1), and corresponding pGWB42 empty vector lines (EV) were also produced for control experiments.

The GPA1-CFP construct was as described in ref. 1. Specifically, the coding region of the enhanced cyanfluorescent protein (Clontech) was inserted in the first loop (between amino acids 97 and 98) of GPA1, and moved into the binary vector pGWB2 (2) which contained the CaMV 35S constitutive promoter. The construct was transformed into *agb1-2* plants by *Agrobacterium*-mediated transformation.

For electrophysiological and physiological assays, all lines were grown under 0.120 mmol m^{-2} s^{-1} of fluorescent light (8 h/16 h day/night cycle) with ~80% relative humidity, and 22°C/20°C day/night temperatures. It was not practicable to simultaneously assay all 10 transgenic genotypes evaluated in this report. Therefore, for all analyses of mutant and overexpressing lines, control experiments on Col were independently repeated on plants grown simultaneously and in the same growth chamber as the particular lines under evaluation.

Preparation of guard cell and mesophyll protoplasts. Guard cell protoplasts for RT-PCR and real-time PCR assays were prepared following the same day large-scale protocol as described (3, 4). Mesophyll cell protoplasts were prepared as described by (4). Guard cell protoplasts for patch clamp analysis were isolated according to the same day small-scale protocol (3, 5).

Patch-clamp analysis. Whole-cell K^+ currents were recorded as described (5) except that the bath solution was adjusted to pH 5.6, and 10 mM Mg·ATP (10 mM from a 0.5 M Mg·ATP stock solution in 0.5 M Tris) was added to the pipette solution immediately before use. The osmolality of all bath and pipette solutions was 540 mmol kg^{-1} or 560 mmol kg^{-1}, respectively. For ABA treatments, protoplasts were pretreated for at least 1.5 h with 50 μM ABA, and 50 μM ABA was also added to the bath solution for K^+ current recording, and to both bath and pipette solution for anion current recording as described previously (6).

RT-PCR and real-time PCR analyses. For RT-PCR analysis of *RGS1* transcripts in guard cell or mesophyll cell protoplasts, the full-length coding region of *RGS1* was amplified by using *RGS1*-specific primers (5′-GAGTGGAGAAGAGAGAGCT-GATATGCT-3′ and 5′-GGTTCCATAGTTTTTGTCCGG-TATACACA-3′). *ACTIN2* primers (5′-GCTGGTTTTGCTG-GTGATGATGC-3′ and 5′-TGTTGGAAGGTGCTGAGG-GATGC-3′) were used as control primers to amplify a portion of the *ACTIN2* cDNA.

Whole leaves of plants were used for total RNA extraction of *YFP-AGB1* overexpressing lines together with knockout mutants and empty vector expressing lines. For RT-PCR analysis, a 1131-bp fragment of *AGB1* cDNA was amplified by using primers (5′-ATGTCTGTCTCCGAGCTCAAAGAACG-3′ and 5′-AATCACTCTCCTGTGTCCTCCAAACG-3′). *ACTIN2* primers (same as indicated above) were also used to amplify *ACTIN2* cDNA for template cDNA estimation.

For RT-PCR analysis of *GPA1* or *AGB1* transcripts in rosette leaves of 4-week-old plants, total RNA was extracted from whole leaves by using TRIZOL reagent (Invitrogen) according to the manufacturer's instructions. Reverse transcription followed by PCR was performed according to the instructions provided with the SuperScript II first-strand synthesis system (Gibco BRL, Life Technologies). For *GPA1*, the forward primer started at 120 base pairs (bp) (forward, 5′-GCTTTTGCTACTTGGTGCTG-3′) and the reverse primer started at 780 bp (reverse, 5′-CCTGTTTTTCTGCTCGTCCT-3′) relative to the *GPA1* cDNA clone. For *AGB1*, the forward primer started at 506 bp (forward, 5′-ATGCCCACCTTATCACCAGTTC-3′); the reverse primer started at 1001 bp (reverse, 5′-CCCAAATC-CAATACAACCTCTCC-3′) in the *AGB1* cDNA clone. For *ACTIN2*, the forward PCR primer started at 61 bp (forward, 5′-GCTGGTTTTGCTGGTGATGATGC-3′); the reverse primer started at 1067 bp (reverse, 5′-TGTTGGAAGGTGCT-GAGGGATGC-3′) in the *ACTIN2* cDNA clone.

For RT-PCR and real-time PCR analyses of *AGB1* and *GPA1* expression in guard cell protoplasts of wild-type and *gpa1* and *agb1* mutants, total RNA from Ws, *gpa1-1*, *gpa1-2*, Col, *agb1-1*, and *agb1-2* was isolated from guard cell protoplasts prepared from just fully expanded leaves. Three hundred ng of total RNA was processed directly into cDNA by reverse transcription with Invitrogen Thermoscript RT-PCR system in a total volume of 20 μl according to the manufacturer's protocol. One μl of cDNA was used as template for subsequent PCR and real-time PCR analyses. For RT-PCR analysis, the full-length coding regions of *GPA1* and *AGB1* were amplified by using *GPA1* primers (5′-ATGGGCTTACTCTGCAGTA-3′and 5′-TCATAAAAGGC-CAGCCTCCAGT-3′), and *AGB1* primers (5′-ATGTCTG-TCTCCGAGCTCAA-3′ and 5′-CTCTCCTGTGTCCTC-CAAA), respectively. *ACTIN2* amplification with primers (5′-GTTGGGATGAACCAGAAGGA-3′ and 5′-GAACCAC-CGATCCAGACACT-3′) was used as control. All oligonucleotides were synthesized by Sigma-Genosys. For real-time analysis, *GPA1* PCR primers (5′-AGAAGTTTGAGGAGTTATAT-TACCAG-3′, and 5′-AAGGCCAGCCTCCAGTAA-3′), and *AGB1* PCR primers (5′-GACGTACTCGGGTGAGCTT-3′ and 5′-GAGCATTCCACACGATTAAT-3′) were used. *ACTIN2* PCR primers (5′-GTTGGGATGAACCAGAAGGA-3′ and 5′-GAGGAGCCTCGGTAAGAAGA-3′) were used as controls to normalize the expression of each gene. All real-time PCR primers were designed to produce 150–200 bp products. PCR amplification and fluorescence detection was accomplished by using DNA Engine Opticon 2 with continuous fluorescence detector (MJ Research). SYBR green was used as the intercalating dye. Primary Cycle Threshold (C_t) values were used to calculate differences in fold changes. Data shown are mean ± SE of three replicates. All values were normalized against the internal control (*ACTIN2*). The reaction was repeated three times. Each time the fold change was calculated against wild type. The fold change for wild type was always set at 1.

Preparation of leaf lysates for immunoblot analyses of GPA1. All procedures were conducted at 4°C. Just fully expanded rosette leaves of 4- to 5-week-old plants were homogenized with Buffer A containing 250 mM Tris-HCl (pH 8.0), 300 mM sucrose, 10 mM EDTA, 1 mM DTT, and 10 μg/ml Protease inhibitor mixture (Roche), 1 mM PMSF, 0.5% (wt/vol) insoluble PVP (Sigma), and sand (−50 + 70 Mesh; Sigma). The homogenate was then centrifuged at 14,000 × *g* for 20 min. 200 μl of the supernatant was recovered as the total fraction, and the remainder was centrifuged at 100,000 × g for 45 min. The supernatant was saved as the soluble fraction. The pellet was resuspended in Buffer B containing 50 mM Tris-HCl (pH 7.4), 120 mM NaCl,

1 mM EDTA-Na_2, 3 mM $MgCl_2$, 1 mM PMSF,10 μg/ml Protease inhibitor mixture, 1 mM DTT, filtered with QIAquik Mini Columns 50 (QIAGEN GmbH) and designated as microsomal proteins. All protein samples were frozen with liquid N_2, and stored at -80°C. Protein concentration was determined by using a Bio-Rad kit based on the Bradford method. Membranes were incubated with primary GPA1-peptide antibody diluted 1:10,000, incubated with secondary anti-rabbit HRP conjugate (Pierce), and then reacted with the HRP substrate of the ECL kit (Pierce) before image development on Kodak x-ray films.

Immunoblot analysis of* AGB1*-overexpressing lines. Leaves from 3-week-old plants were used for protein extraction. Leaves were ground in liquid nitrogen and incubated for 15 min in SDS reducing buffer [62.5 mM Tris-HCl, pH 6.8, 20% glycerol, 2% SDS, 5% β-mercaptoethanol, and 0.025% (wt/vol) bromophenol blue] at room temperature. The homogenates were centrifuged at 21,000 $\times$ *g* at 4°C for 15 min and the supernatants were boiled for 5 min before loading onto SDS/PAGE gels. Protein assay dye (Bio-Rad Inc.) was used for protein quantification. For the Western blot, GFP antibody was used (Living Colors GFP monoclonal antibody; Clontech) as the primary antibody and anti-Mouse IgG HRP conjugate was used as the secondary antibody (Promega). The SuperSignal West Pico Chemiluminescent substrate of HRP (Pierce) was used for photodevelopment.

Stomatal bioassays. Fully expanded young leaves from 4-week-old plants were excised for stomatal bioassays. For stomatal opening assays, leaves were kept in opening solution (10 mM KCl, 7.5 mM iminodiacetic acid, 10 mM Mes-KOH, pH 6.15) with their adaxial surface upward in the dark for 2.5 h to close the stomata. Before transfer to light (0.450 mmol m^{-2} s^{-1}), ABA (or same volume of ethanol as solvent control) was added and the leaves were kept in light for another 2.5 h before measurement. For assays of stomatal closure, leaves were kept in the light in closure solution (20 mM KCl, 1 mM $CaCl_2$, 5 mM Mes-KOH, pH 6.15) for 2.5 h and then ABA or ethanol control was added and leaves were maintained in light for another 2.5 h before measurement. For the measurement of stomatal apertures, abaxial leaf epidermes were peeled and photographed at 400× total magnification, and stomatal apertures were subsequently measured with ImageJ open access software (version 1.37). Each stomatal aperture assay was performed with at least three independent replicates, and at least 150 stomatal apertures were measured in each replicate. Student's *t* test was used to compare the ABA effect, and *P* values $\leq$0.01 were considered significant differences.

Results. ***RT-PCR of* AGB1 *and Western blotting of AGB1 in AGB1-overexpressing plants.*** To confirm genotypes of the plant lines used for experiments, we performed RT-PCR on *agb1-1, agb1-2, OX5, OX6* and empty vector control lines (*EV1* and *EV3*) together with wild type. As shown in supporting information (SI) Fig. S1*A*, there was no *AGB1* expression in *agb1-2* mutants. Empty vector lines (*EV1* and *EV3*) showed the same level of *AGB1* transcript as Col, and overexpressing lines (OX5 and OX6) indeed exhibited more *AGB1* transcript. RT-PCR with 35 cycles (not shown) instead of 25 cycles amplified a faint band from *agb1-1* but not *agb1-2*, as expected based on results previously reported by Lease *et al.* (7). Because we were unsuccessful in generating AGB1 antibody, despite numerous attempts, we used the GFP antibody to evaluate YFP-AGB1 overexpressing lines. As shown in Fig. S1*B*, YFP was highly expressed in *EV1* and *EV3* plant lines and the fusion protein, YFP-AGB1, was highly expressed in *OX5* and *OX6* lines. These plants were used for further physiological analyses.

K^+ currents of AGB1-overexpressing plants show a wild-type response to subsaturating ABA concentrations. To evaluate whether there might be a difference in ABA sensitivity between Col and the AGB1 overexpressing lines OX5 and OX6 that was not revealed at 50 μM ABA, we also used lower ABA concentrations. As shown by the *I–V* curves in Fig. S2, at 20 μM ABA (Fig. S2*A*) and 5 μM ABA (Fig. S2*B*), responses of OX5 and OX6 plants were still indistinguishable from those of Col wild-type plants.

AGB1 overexpression restores wild-type ABA effects on stomatal opening and K_{in} currents to agb1 mutants. To further evaluate *AGB1* function in the regulation of stomatal opening and inward K^+ currents, we transformed full-length *AGB1* cDNA driven by the CaMV 35S promoter into *agb1-2* and *gpa1-4 agb1-2* double mutants to check whether *AGB1* expression suppresses the mutant phenotypes. As shown in Fig. S2*A*, *AGB1* transcript was overexpressed to some extent in both *agb1-2* and *gpa1-4 agb1-2* double mutant backgrounds. This *AGB1* expression did rescue ABA sensitivity of stomatal opening and inward K^+ channel inhibition in the *agb1-2* single mutant (Fig. S3 *B* and *C*). However, *AGB1* expression did not suppress the mutant phenotype of the *gpa1-4 agb1-2* double mutant for either ABA sensitivity of stomatal opening or K_{in} channel regulation (Fig. S3 *B* and *C*). This result is consistent with the fact that these plants were still lacking the GPA1 Gα subunit, whose knockout is known to confer ABA hyposensitivity to these processes (5).

RT-PCR of* RGS1 *in guard cell or mesophyll cell protoplasts. To evaluate a possible functional role of RGS1 in controlling guard cell function, we tested the transcript levels of *RGS1* in guard cell and mesophyll cell protoplasts. As shown in Fig. S4, the *RGS1* transcript is expressed in guard cells, and is found at a level comparable to its expression in mesophyll cells.

rgs1 ***null mutation affects kinetics of voltage activation.*** Accelerated kinetics of K_{in} current response following voltage activation were observed in the *rgs1* mutants under control conditions (Fig. S5); this phenomenon was not observed in any of the other mutant genotypes (data not shown). K_{in} deactivation kinetics were unaltered in *rgs1* mutants (data not shown).

GPA1 expression in rosette leaves. GPA1 was present in Ws and Col wild-type samples where it was mainly localized to the crude membrane fraction. As expected, GPA1 was not detected in any fractions of the *gpa1* null mutant lines (Fig. S6).

***RT-PCR, real-time PCR of* GPA1 *and* AGB1.** To address whether GPA1 and AGB1 work in the same pathway, it is helpful to test whether GPA1 affects *AGB1* expression, or vice versa. We conducted RT-PCR analyses with total RNA extracted from either whole leaves (Fig. S7*A*) or guard cell protoplasts (Fig. S7 *B* and *C*). We found that *AGB1* was expressed at a similar level among two *gpa1* mutant lines and Ws wild-type plants, and *GPA1* was expressed at a similar level among two *agb1* mutant lines and Col wild-type plants. Note that in Fig. S3 *A* and *B*, *AGB1* product was not present in the *agb1-2* mutant but was present in the *agb1-1* point mutant, although at a lower level than in wild-type (cf. ref. 7). As shown, *GPA1* product was absent in both *gpa1* null mutants. We further performed real-time PCR analyses to quantify the transcripts, starting with total RNA isolated from highly purified (~98% pure on a cell basis) guard cell protoplasts. *AGB1* transcript levels in guard cells were comparable among the two *gpa1* mutant lines and Ws wild-type plants whereas the *GPA1* transcript levels were similar in the two *agb1* mutant lines and Col wild-type plants (Fig. S7*C*).

RGS1 ***mutations do not alter steady-state ABA-inhibition of stomatal opening.*** To evaluate whether RGS1 is involved in ABA-regulation of stomatal opening, we performed stomatal aperture assays on Col wild-type and two independent *RGS1* loss-function mutants, *rgs1-1* and *rgs1-2*. *rgs1-1* and *rgs1-2* plants exhibited wild-type ABA inhibition of stomatal opening (Fig. S8), consistent with their wild-type K^+ current–voltage characteristics (Fig. S5).

1. Chen JG, *et al.* (2003) A seven-transmembrane ZGS protein that modulates plant cell proliferation. *Science* 301:1728–1731.
2. Nakagawa T, *et al.* (2007) Development of series of Gateway binary vectors, pGWBs, for realizing efficient construction of fusion genes for plant transformation. *J Biosci Bioeng* 104:34–41.
3. Pandey S, Wang XQ, Coursol S, Assmann SM (2001) Preparation and applications of *Arabidopsis thaliana* guard cell protoplasts. *New Phytol* 153:517–526.
4. Coursol S, *et al.* (2003) Sphingolipid signalling in *Arabidopsis* guard cells involves heterotrimeric G proteins. *Nature* 423:651–654.
5. Wang XQ, Ullah H, Jones AM, Assmann SM (2001) G protein regulation of ion channels and abscisic acid signaling in *Arabidopsis* guard cells. *Science* 292:2070–2072.
6. Pei ZM, Kuchitsu K, Ward JM, Schwarz M, Schroeder JI (1997) Differential abscisic acid regulation of guard cell slow anion channels in *Arabidopsis* wild-type and *abi1* and *abi2* mutants. *Plant Cell* 9:409–423.
7. Lease KA, *et al.* (2001) A mutant *Arabidopsis* heterotrimeric G-protein β subunit affects leaf, flower, and fruit development. *Plant Cell* 13:2631–2641.
8. Karimi M, Inzé D, Depicker A (2002) GATEWAY vectors for *Agrobacterium*-mediated plant transformation. *Trends Plants Sci* 7:193–195.

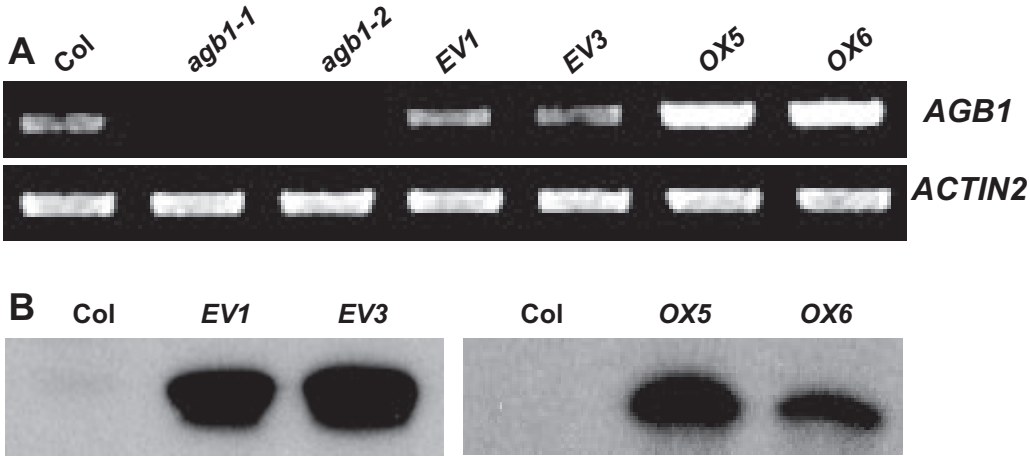

Fig. S1. RT-PCR and immunoblot analyses of AGB1 overexpressing plants. (*A*) Reverse transcription PCR (RT-PCR) of Col, *AGB1* knockout mutants (*agb1-1*, *agb1-2*), pGWB42 empty vector (pGWB2-35S-YFP) lines (*EV1*, *EV3*), and AGB1 overexpressing (pGWB2-35S-YFP-ABG1) lines (OX5, OX6). (*B*) Western blot of empty vector lines (*EV1*, *EV3*) and AGB1 overexpressing lines (*OX5*, *OX6*) by using GFP antibody.

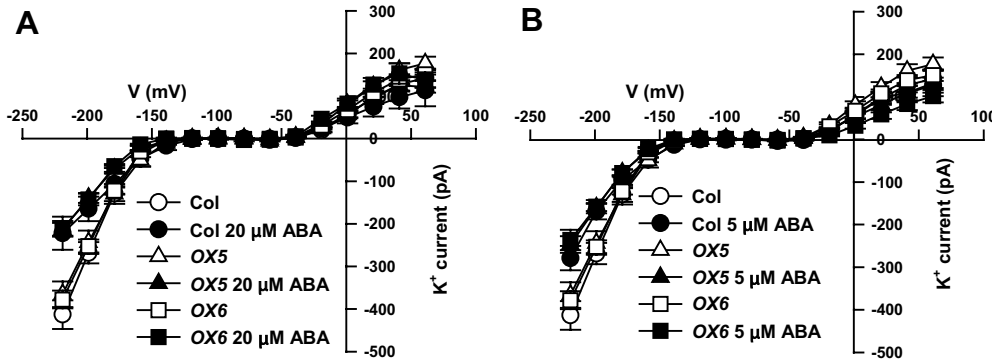

Fig. S2. Wild-type ABA-inhibition of inward K^+ currents in AGB1 overexpressing lines is maintained even at low ABA concentrations. (*A*) *I–V* curves (mean ± SE) of time-activated whole-cell K^+ currents with or without 20 μM ABA treatment. $n = 8, 7$ cells for control and 20 μM ABA treatment of Col; $n = 6, 6$ cells for *OX5*; $n = 8, 8$ cells for *OX6*. (*B*) *I–V* curves (mean ± SE) of time-activated whole-cell K^+ currents with or without 5 μM ABA treatment. $n = 8, 7$ cells for control and 20 μM ABA treatment of Col; $n = 6, 5$ cells for *OX5*; $n = 8, 4$ cells for *OX6*.

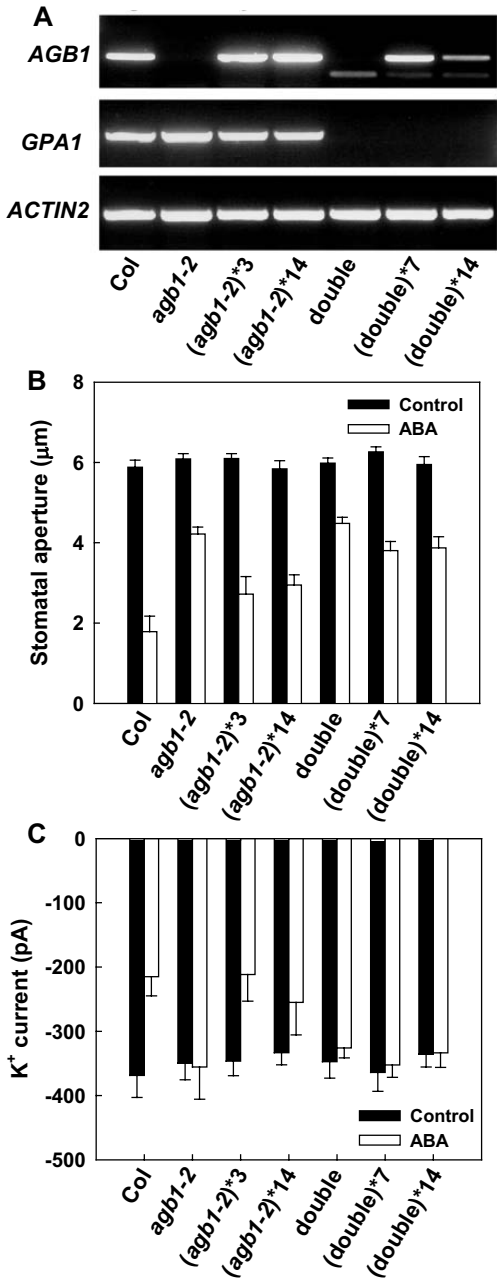

Fig. S3. *AGB1* expression restores wild-type ABA effects on stomatal opening and K_{in} currents in *agb1* mutants but not in *gpa1 agb1* double mutants. (*A*) *AGB1* and *GPA1* transcript levels in various lines. For AGB1 complementation experiments, full-length *AGB1* cDNA coding regions were cloned into binary vector pB2GW7 (8) under control of the CaMV 35S promoter for *Agrobacterium tumefaciens*–mediated transformation of *agb1-2* and *gpa1-4 agb1-2* double mutant. (*agb1-2*)*3 and (*agb1-2*)*14 are two independent *AGB1* overexpressing lines in *agb1-2* background, (double)*7 and (double)*14 are two independent *AGB1* overexpressing lines in *gpa1-4 agb1-2* double mutant background. (*B*) Stomatal opening assay. Wild-type ABA (50 μM) inhibition of stomatal opening was restored in (*agb1-2)*3* and (*agb1-2)*14* complemented lines (Student's *t* test, $P > 0.05$ as compared with Col) but hyposensitivity of ABA inhibition of stomatal opening was retained in (*double)*7* and (*double)*14* lines ($P \leq 0.05$ as compared with Col). +ABA for (*double)*7* and (*double)*14* was not significantly different from +ABA for the *gpa1-4 agb1-2* double mutant ($P > 0.05$, Student's *t* test). (*C*) Electrophysiology of K_{in} currents in *Arabidopsis* guard cell protoplasts. Wild-type ABA (50 μM) inhibition of K_{in} currents, quantified in the figure at -219 mV was restored in (*agb1-2)*3* and (*agb1-2)*14* complemented lines (Student's *t* test, $P > 0.05$ as compared with Col) but hyposensitivity of ABA inhibition of K_{in} currents was retained in (*double)*7* and (*double)*14* lines ($P \leq 0.05$ as compared with Col). +ABA for (*double)*7* and (*double)*14* was not significantly different from +ABA for the *gpa1-4 agb1-2* double mutant ($P > 0.05$, Student's *t* test). Cell numbers: Col-control (11), Col-ABA (9), *agb1-2*-control (9), *agb1-2*-ABA (8), (*agb1-2*)*3-control (14), (*agb1-2*)*3-ABA (9), (*agb1-2*)*14-control (10), (*agb1-2*)*14-ABA (6), double-control (11), double-ABA (8), (double)*7-control (9), (double)*7-ABA (10), (double)*14-control (7), (double)*14-ABA (7). 50 μM ABA was used for both K_{in} current and stomatal aperture assays. The protocols for whole-cell recording of K_{in} currents and measurement of stomatal apertures are as described in Methods in *SI Text* except that measurement of stomatal apertures was performed by using an ocular micrometer. Each assay was performed with at least three independent replicates, and at least 30 stomatal apertures were measured in each replicate.

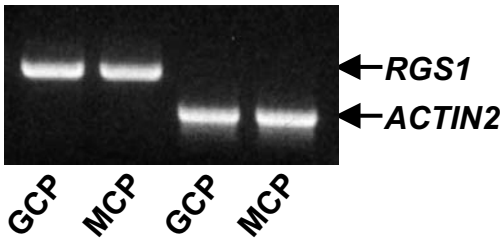

Fig. S4. RT-PCR analysis of *RGS1* expression guard cell or mesophyll cell protoplasts of wild-type (Ws) plants. Lanes 1 or 2 indicate the relative transcript levels of *RGS1* in guard cell protoplasts (GCP) or mesophyll cell protoplasts (MCP), whereas lanes 3 or 4 indicate the relative cDNA amounts of *ACTIN2* transcripts in guard cell protoplasts (GCP) or mesophyll cell protoplasts (MCP).

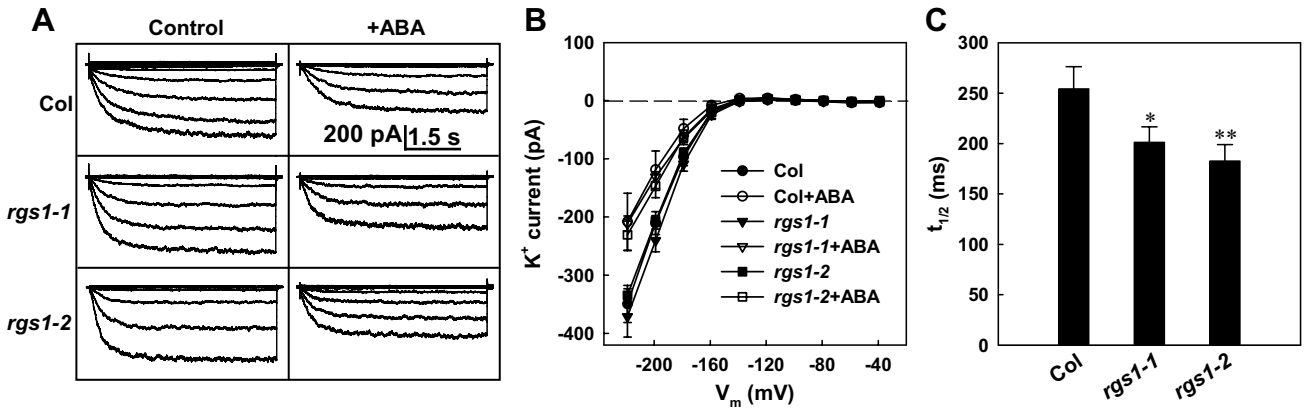

Fig. S5. *rgs1* mutation does not alter ABA-sensitivity of K_{in} currents but accelerates voltage-activation. (*A*) Whole-cell recordings of guard-cell K_{in} currents with or without 50 μM ABA. (*B*) *I–V* curves (mean ± SE) of time-activated whole-cell K_{in} currents. $n = 8$, 12 cells for control and ABA treatment of Col; $n = 8$, 8 cells for *rgs1-1*; $n = 15$, 14 cells for *rgs1-2*. (*C*) Half-activation time (mean ± SE) of K_{in} currents. $n = 8$, 12 cells for control and ABA treatment of Col; $n = 8$, 8 for *rgs1-1*; $n = 15$, 14 for *rgs1-2*. * and **, significantly different from Col at $P \leq 0.05$ or 0.01, respectively, by Student's *t* test.

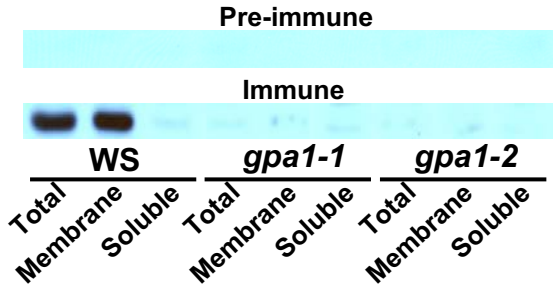

Fig. S6. Immunoblot analysis of GPA1 in Ws and two *gpa1* mutants. GPA1 is expressed in Ws wild-type but not in *gpa1* mutant lines, and GPA1 is mainly localized to membranes (*Lower*). *Upper* shows a Western blot with corresponding preimmune serum at the same dilution as for immune serum.

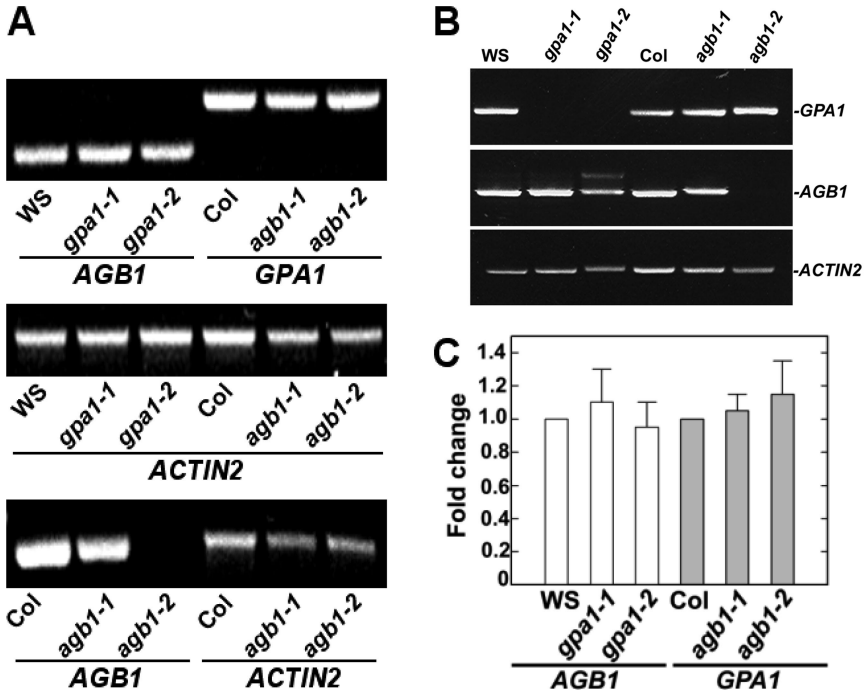

Fig. S7. RT-PCR and real-time PCR analyses of *AGB1* and *GPA1* expression in rosette leaves and guard cell protoplasts of wild-type and mutant (*agb1* and *gpa1*) lines. (*A*) RT-PCR analysis of *AGB1* and *GPA1* expression in leaf tissue. (*Upper*) *AGB1* transcript levels in Ws and *gpa1* mutants, and Col and *agb1* mutants. *AGB1* transcript level is comparable among Ws (lane 1) and *gpa1-1* and *gpa1-2* mutants in the Ws ecotypic background (lanes 2 and 3), whereas *GPA1* transcript level is comparable among Col (lane 4) and *agb1-1* and *agb1-2* mutants in the Col ecotypic background (lanes 5 and 6). (*Middle*) *ACTIN2* transcripts indicate relative cDNA amounts. (*Lower*) *AGB1* and *ACTIN2* transcript levels in Col and two Col *agb1* mutants. The portion of *AGB1* transcript was detected in the leaves of Col wild-type (lane 1) and an EMS-generated *agb1-1* mutant (lane 2) but not in the leaves of the *agb1-2* knockout mutant (lane 3). For all panels, *AGB1* and *GPA1* primers flanked the respective T-DNA insertion sites. (*B*) RT-PCR analysis of *GPA1* and *AGB1* transcript levels in guard cell protoplasts. (*Top*) *GPA1* transcript levels in Ws and *gpa1* mutants, and Col and *agb1* mutants. *GPA1* transcript is absent in the two *gpa1* mutants, but its level is comparable among Col and the two *agb1* mutants. (*Middle*) *AGB1* transcript levels in Ws and *gpa1* mutants, and Col and *agb1* mutants. *AGB1* transcript level is comparable among Ws and two *gpa1* mutants. AGB1 transcript was detected in both Col and the *agb1-1* point mutant but was absent in the *agb1-2* knockout mutant. The full-length coding regions of *GPA1* and *AGB1* were amplified. (*Bottom*) *ACTIN2* transcript levels in Ws and *gpa1* mutants, and Col and *agb1* mutants, showing comparable amounts. (*C*) Real-time PCR analysis of *AGB1* transcript in *gpa1* mutant background guard cell protoplasts, and *GPA1* transcript in *agb1* mutant background guard cell protoplasts. Fold changes against wild types are shown as relative levels of *AGB1* or *GPA1* transcript. Data presented are mean ± SE of three replicates.

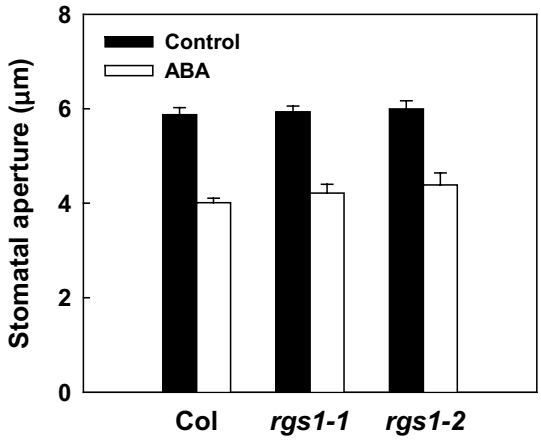

Fig. S8. Wild-type ABA-inhibition of stomatal opening in *rgs1* mutants. *RGS1* mutations in *rgs1-1* and *rgs1-2* did not alter ABA (50 μM) inhibition of stomatal opening (mean $\pm$ SE). Stomatal aperture assay was performed as described in the legend of Fig. S3.